Toxicology in Vitro 59 (2019) 238–245

Contents lists available at ScienceDirect

Toxicology in Vitro

journal homepage: www.elsevier.com/locate/toxinvit

Gut microbial transformation of the dietary mutagen MeIQx may reduce exposure levels without altering intestinal transport

Jianbo Zhang[a,1], Michael T. Empl[b,2], Mirjam Schneider[a], Bernd Schröder[c], Julita Stadnicka-Michalak[d,e], Gerhard Breves[c], Pablo Steinberg[b,*,3], Shana J. Sturla[a,*]

[a] Department of Health Sciences and Technology, ETH Zürich, Zürich, Switzerland
[b] Institute for Food Toxicology, University of Veterinary Medicine Hannover, Hannover, Germany
[c] Department of Physiology, University of Veterinary Medicine Hannover, Hannover, Germany
[d] Eawag, Dübendorf, Switzerland
[e] School of Architecture, Civil and Environmental Engineering, EPF Lausanne, Switzerland

ARTICLE INFO

Keywords:
Heterocyclic aromatic amines
MeIQx
MeIQx-M1
Intestinal uptake
Physiologically based pharmacokinetic modeling
HepaRG cells

ABSTRACT

The mutagen and probable human carcinogen 2-amino-3,8-dimethylimidazo[4,5-*f*]quinoxaline (MeIQx) is metabolized in the colon to 9-hydroxyl-2,7-dimethyl-7,9,10,11-tetrahydropyrimido[2′,1′:2,3]imidazo[4,5-*f*]quinoxaline (MeIQx-M1) by conjugation with microbially generated acrolein. However, whether this microbiota-controlled process alters systemic exposure and hepatotoxicity of MeIQx remains unclear. The physiological relevance of this microbial transformation on the systemic exposure of MeIQx was investigated using an in vitro-in vivo extrapolation approach. To address whether microbial transformation influences intestinal transport of MeIQx, the intestinal uptake of MeIQx and its metabolite MeIQx-M1 was quantified using Ussing chambers mounted with different intestinal segments from male Fischer 344 rats. Up to 0.4% of both MeIQx and MeIQx-M1 were transported from the mucosal side to the serosal side of intestinal tissue within 90 min, suggesting that the intestinal uptake of both compounds is similar. With the uptake rates of both compounds, physiologically based pharmacokinetic (PBPK) modeling of the fate of MeIQx in the human body including microbial transformation of MeIQx was performed. Results indicate for the first time that high levels of microbe-derived acrolein would be required to significantly reduce systemic exposure of MeIQx in humans. Finally, neither MeIQx nor MeIQx-M1 were cytotoxic towards human liver HepaRG cells at dietary or higher concentrations of MeIQx. In summary, these findings suggest that gut microbial transformation of heterocyclic amines has the potential to influence systemic human exposure to some extent, but may require significant gut microbial production of acrolein and that further investigations are needed to understand physiological levels of acrolein and competing biotransformation pathways.

1. Introduction

The association of well-cooked red meat with increased colorectal cancer risk is in part attributed to exposure to carcinogenic chemicals such as heterocyclic aromatic amines (HCAs; Ushiyama et al., 1991; Sinha et al., 2001; Bouvard et al., 2015) like 2-amino-1-methyl-6-phenylimidazo[4,5-*b*]pyridine (PhIP) (Felton et al., 1986), 2-amino-3,8-dimethylimidazo[4,5-*f*]quinoxaline (MeIQx) (Jägerstad et al., 1984), and 2-amino-3-methylimidazo[4,5-*f*]quinoline (IQ) (Kasai et al., 1980). Upon metabolic activation, HCAs form DNA adducts (Nauwelaers et al., 2011), are mutagenic (Kim and Guengerich, 2005; Rendic and Guengerich, 2012; Sugimura, 1988), induce malignant cell transformation (Pfau et al., 1999) as well as mutations in oncogenes of rodent and human fibroblasts (Sugimura et al., 2004), and form tumors in multiple organs in rodent models (Ito et al., 1991; Kato et al., 1988; Ohgaki et al., 1987; Sugimura et al., 2004). We recently showed that complex human-derived gut microbial communities can reduce the mutagenicity of HCAs by conversion to their acrolein conjugates (i.e. conversion of MeIQx to 9-hydroxyl-2,7-dimethyl-7,9,10,11-tetrahydropyrimido[2′,1′:2,3]imidazo[4,5-*f*]quinoxaline or MeIQx-M1)

* Corresponding authors.
E-mail addresses: pablo.steinberg@mri.bund.de (P. Steinberg), sturlas@ethz.ch (S.J. Sturla).
[1] Current address: Department of Biological Engineering, Massachusetts Institute of Technology, Cambridge, MA, United States.
[2] Current address: Fraunhofer Institute for Toxicology and Experimental Medicine ITEM, Nikolai-Fuchs-Straße 1, 30625, Hannover, Germany.
[3] Current address: Max Rubner-Institut, Federal Research Institute of Nutrition and Food, Karlsruhe, Germany.

https://doi.org/10.1016/j.tiv.2019.04.004
Received 22 August 2018; Received in revised form 27 March 2019; Accepted 3 April 2019
Available online 04 April 2019

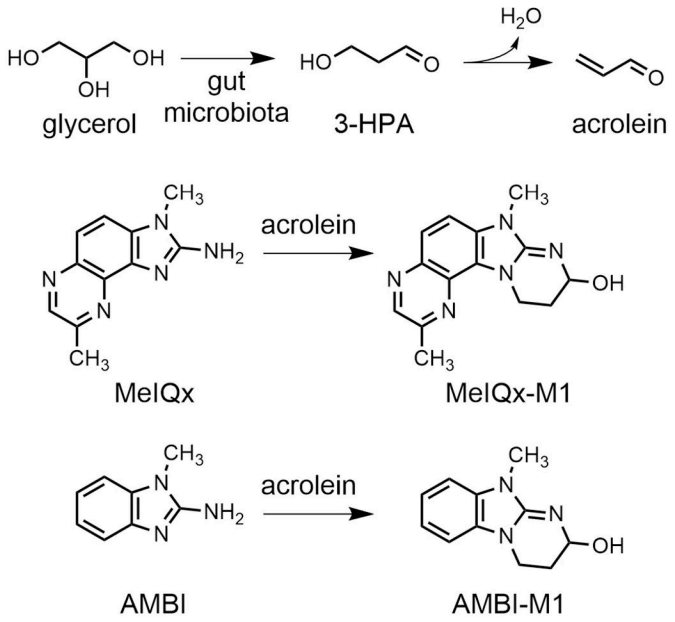

Fig. 1. Gut microbe-derived acrolein and its reaction with MeIQx as well as AMBI forming MeIQx-M1 and AMBI-M1, respectively. AMBI and AMBI-M1 were used as internal standards. AMBI: 2-amino-3-methyl benzimidazole; AMBI-M1: 2-hydroxyl-10-methyl-2,3,4,10-tetrahydrobenzo[4,5]imidazo[1,2-*a*] pyrimidine; MeIQx: 2-Amino-3,8-dimethylimidazo[4,5-*f*]quinoxaline; MeIQx-M1: 9-hydroxyl-2,7-dimethyl-7,9,10,11-tetrahydropyrimido[2′,1′:2,3]imidazo [4,5-*f*]quinoxaline.

(Fig. 1) (Zhang et al., 2017). Similar microbial metabolites were observed for other HCAs, including PhIP (Fekry et al., 2016; Vanhaecke et al., 2006), IQ (Zhang et al., 2017) and 2-amino-9H-pyrido[2,3-*b*] indole (AαC) (Beer et al., 2017). However, our understanding of this process raises several questions concerning its physiological relevance of this process and whether it can impact on the disposition of HCAs in humans.

The mechanism of microbial conversion of MeIQx to MeIQx-M1 is well established. Bacteria that harbor the *pduCDE*-gene encoding for the glycerol to 3-hydroxypropionaldehyde (3-HPA)-catalyzing enzyme glycerol/diol dehydratase (De Angelis et al., 2014; Engels et al., 2016; Fekry et al., 2016), such as *Enterococcus* spp., *Lactobacillus reuteri* (Vanhaecke et al., 2008b), *Lactobacillus rossiae*, and *Eubacterium hallii* (Fekry et al., 2016; Zhang et al., 2017), are responsible for this metabolic transformation. 3-HPA chemically decomposes to release acrolein, which then binds to HCAs to form HCA-M1 metabolites (Beer et al., 2017; Engels et al., 2016; Zhang et al., 2017). The transformation blocks the metabolic activation site of HCAs, thereby avoiding their capacity to bind DNA and thereby significantly reducing their mutagenicity (Vanhaecke et al., 2008a; Zhang et al., 2017). Bacteria-mediated glycerol conjugation has therefore been proposed as a detoxification pathway for HCAs in the human lower digestive tract, however, the physiological relevance of this process depends on whether HCA and/or HCA-M1 are absorbed.

It has been shown that gut microbial transformation, due to a potential alteration of absorption, can change the systemic levels of drugs and toxicants and thereby their efficacy and toxicity, respectively (Behr et al., 2017; Haiser et al., 2013; Spanogiannopoulos et al., 2016). In the case of HCAs, Humblot et al. (2007) have shown that bacterial hydrolysis of IQ-glucuronide increased urine levels of IQ in rats mono-colonized with β-glucuronidase-positive *Escherichia coli*. MeIQx has been quantified in plasma of healthy individuals and the clearance rates were highly variable among individuals (Malfatti et al., 2016), highlighting the importance of understanding the currently unknown influence of microbial conversion on intestinal transport and toxicokinetics of MeIQx and MeIQx-M1.

The aim of this study was to investigate how bacterial transformation of MeIQx may lead to a physiologically relevant reduction of the systemic exposure to MeIQx. We determined the capacity of rat intestinal tissue to transport MeIQx and MeIQx-M1. This information led us to develop a physiologically based pharmacokinetic (PBPK) model to describe the impact of MeIQx-M1 formation on the disposition of MeIQx. Finally, we evaluated the toxicological relevance of intestinal uptake by characterizing the cytotoxic potential of MeIQx and MeIQx-M1 towards a human liver cell line in vitro. The relevance of the findings is discussed in the context of whether microbial transformation may modulate systemic HCA exposure in humans.

2. Materials and methods

2.1. Chemicals

MeIQx was purchased from Chemie Brunschwig (Basel, Switzerland). Acrolein, 2-amino-1-methylbenzimidazole (AMBI), and the constituents of the culture media were purchased from Sigma-Aldrich (Buchs, Switzerland). HPLC-grade acetonitrile and methanol were purchased from Merck (Darmstadt, Germany) and Sigma-Aldrich, respectively. Formic acid was purchased from Fisher Scientific (Geel, Belgium), and water was purified with a Milli-Q Integral Water Purification System (Millipore, Billerica, MA, USA). 9-Hydroxyl-2,7-dimethyl-7,9,10,11-tetrahydropyrimido[2′,1′:2,3]imidazo[4,5-*f*]quinoxaline (MeIQx-M1) and 2-hydroxyl-10-methyl-2,3,4,10-tetrahydrobenzo[4,5]imidazo[1,2-*a*]pyrimidine (AMBI-M1) were prepared by reaction of MeIQx or AMBI with acrolein using a procedure described elsewhere (Zhang et al., 2017).

2.2. Animals

Seven to nine weeks old male Fischer 344 rats with a body weight of 239–273 g (Fig. S1) were obtained from Charles River (Sulzfeld, Germany). They were housed for 7 days in the animal facility of the Department of Physiology at the University of Veterinary Medicine Hannover (Hannover, Germany) prior to sacrifice. During this period, the animals had free access to water and standard rodent maintenance feed and were kept under a 12/12 h light/dark lighting regime. The study was performed under approval no. 33.9-42502-05-12A219 of the Animal Welfare Service of the Lower Saxony State Office for Consumer Protection and Food Safety (LAVES; Oldenburg, Germany).

2.3. Preparation of the intestinal segments and Ussing chamber experiments

Intestinal segments were prepared according to the method described by Tóth (2007). Briefly, all rats were sacrificed using CO_2. The whole gut was removed and then kept in ice-cold Krebs-Henseleit solution continuously gassed with carbogen (95% O_2, 5% CO_2) for approximately 5 min. Then, they were prepared for the Ussing chamber experiments. The initial part of the colon was thereby defined as the beginning of the large intestine connected to the caecum (identified by a characteristic v-forming pattern along the mesentery artery). The jejunum was defined as the segment distal to the ligament of Treitz and was removed completely until the beginning of the ileum. The specified location of different segments used for the experiments was as follows: The duodenal sample was taken 1 cm below the pylorus, the proximal jejunal sample 15 cm distal of the duodenum, the distal jejunal sample 10 cm proximal of the ileum, the ileal sample directly proximal to the caecum and the caecal sample from the *corpus caeci*. The tissue excised up to 3 cm distal to the junction of the caecum and the colon was defined as proximal colon, tissue immediately distal to this segment as distal colon, and the remaining segment as rectum. Once the gut was removed and segmented, the *tunica serosa* and *tunica muscularis* of the tissue segments were removed by stripping on ice, prior to them being

mounted into the Ussing chambers. The area of a single chamber aperture was 0.5 cm^2 for all tissues as described in detail elsewhere (Breves et al., 2000). Two silicon rings were used to ensure a good connection between the two halves of the chambers and to prevent damage to the epithelium.

The Ussing chamber experiments were performed using procedures described by Breves et al. (2000) and Nicken et al. (2015). Briefly, after tissues were mounted into the Ussing chambers, the whole system was equilibrated with carbogen gas for 30 min. Thereafter, 10 mM stock solutions of MeIQx or MeIQx-M1 were added to the mucosal compartments (final concentration: 10 µM). One and 90 min after the addition of the compounds (longer incubation times were not tested because of tissue deterioration), samples for LC-MS analysis (400 µl) were removed from each compartment and immediately snap-frozen in liquid nitrogen. In order to determine unspecific binding of MeIQx and MeIQx-M1 to the surface of the Ussing chambers, a silicone membrane was additionally mounted. The components of the buffer solutions added to the Ussing chambers are listed in Table S1.

2.4. Quantification of MeIQx and MeIQx-M1 in the mucosal and serosal compartments of the Ussing chambers

The concentration of MeIQx and MeIQx-M1 was measured by nanoLC-mass spectrometry using a nanoACQUITY UPLC™ system (Waters Corporation, Milford, MA, USA) equipped with a capillary column and a triple quadruple (QqQ) mass spectrometer. The capillary column (75 µm × 10 cm D × l, 15 µm orifice) was hand-packed using a commercially available fused-silica emitter (New Objective, Woburn, MA; USA) with 5 µm Luna C18-bonded separation media (Phenomenex, Torrance, CA, USA). The mobile phase A consisted of 0.1% formic acid in ultrapure water, while the mobile phase B consisted of 0.1% formic acid in acetonitrile. The separation was achieved using the following gradients: 0–5 min, flow rate (FL) 1 µl min^{-1}, isocratic 13% B; 0–5.5 min, FL convex 1–0.3 µl min^{-1}, isocratic 13% B; 5.5–6 min, FL 0.3 µl min^{-1}, linear 13–25% B; 6–8 min, FL 0.3 µl min^{-1}, isocratic 25% B; 8–8.5 min, FL 0.3 µl min^{-1}, linear 25–98% B; 8.5–9 min, linear 0.3–1 µl min^{-1}, isocratic 98% B; 9–11 min, FL 1 µl min^{-1}, isocratic 98% B. The column was then returned to the initial conditions and re-equilibrated for 5 min. The eluent was ionized by nano-electro spray ionization (nano-ESI) in the positive mode and the compounds were monitored by a QqQ mass spectrometer with the following transition reactions: MeIQx, 214 → 199, 214 → 172; MeIQx-M1, 270 → 252, 270 → 214; AMBI, 148 → 133; AMBI-M1, 204 → 186, 204 → 148 (Fig. S2).

2-Amino-3-methyl benzimidazole (AMBI) and 10-methyl-2,3,4,10-tetrahydrobenzo[4,5]imidazo[1,2-*a*]pyrimidin-2-ol (AMBI-M1) (Fig. 1) were added to samples as internal reference standards for MeIQx and MeIQx-M1, respectively. The mixture was concentrated under vacuum, the residue was dissolved in acetonitrile diluted appropriately with water and filtered using a 0.2 µm polyvinylidene difluoride membrane. The linear range of the calibration curve was 1–100 nM (Fig. S3). The limit of quantification for this method was determined to be 1 nM for both MeIQx and MeIQx-M1 based on a signal to noise ratio of 10.

2.5. Calculation of the apparent permeability coefficient (P_{app}) for MeIQx and MeIQx-M1

The apparent permeability coefficient for intestinal transport was estimated according to the following equation (Yee, 1997):

$$P_{app} = \frac{\Delta C_s \times V_s}{\Delta t \times A \times C_{m0} \times V_m}$$

where V_s and V_m = volume of medium (in l) perfusing the serosal and mucosal reservoir, respectively, ΔC_s = concentration change (nmol l^{-1}) in the serosal reservoir at the time interval between t_2 and t_1, Δt = time interval (in seconds) between t_2 and t_1, A = area of the tissue/membrane = 0.5 cm^2, P_{app} = unidirectional flux (in nmol cm^{-1} h^{-1}) from mucosa to serosa, C_{m0} = initial concentration (in nmol l^{-1}) in the mucosal reservoir.

2.6. Physiologically based pharmacokinetic kinetic (PBPK) modeling

To evaluate the influence of the bacteria-derived acrolein-mediated metabolic transformation of MeIQx on its disposition in humans, we developed a PBPK model with perfusion rate-limited kinetics (Fig. S4). The model developed in this study was adapted from PBPK models reported by Al-Malahmeh et al. (2017) for rats and humans. The model consists of six compartments, lung, liver, gut tissue, adipose tissue (fat), richly perfused tissue, and slowly perfused tissue, connected by the systemic circulation. Physiological parameters (i.e. body weight, tissue volumes, cardiac output, and tissue blood flows) of individuals were derived from literature (Table S2; Brown et al., 1997). Partition coefficients describing the distribution of MeIQx in different compartments were estimated based on the method described by DeJongh et al. (1997); Table S3). The uptake of MeIQx from the gut could be described as a first order kinetic process, assuming direct uptake by the liver with an absorption rate constant k_a (Table S4). The catalytic parameters of glucuronidation, sulfation, and oxidation in the liver were derived from in vitro data obtained in the course of the incubation of substrates with microsomal/cytosol proteins, i.e. uridine 5′-diphospho-glucuronosyltransferase (UGT), sulfotransferase, and cytochrome P450 enzymes (Table S2; Ozawa et al., 1995; Malfatti and Felton, 2004; Zhou et al., 2004). The rate of formation of MeIQx-M1 is a second order reaction of MeIQx with acrolein and the second order rate constant was derived from the direct reaction of acrolein with MeIQx as previously reported (Zhang et al., 2017). The mass balance equations were expressed as differential equations and solved using Berkeley Madonna (Macey and Oster, UC Berkeley, CA, USA) with Rosenbrock's algorithm for stiff systems (version 8.3.18) or Euler's method (version 9.1.9). To test the impact of acrolein on the plasma concentration of MeIQx, we applied the PBPK model to fit the above-mentioned parameters (Tables S2–S4) to the measured plasma concentration in the presence of acrolein. Thereafter, these fitted parameters were used to simulate the impact of acrolein on the MeIQx plasma concentration by comparing the plasma level of MeIQx in the presence of acrolein with those in the absence of this compound. More details on modeling equations, codes, sensitivity analysis, and performance evaluation are available in the Supplementary Information.

2.7. Cytotoxicity assay

HepaRG™ cells (Biopredic International, Rennes, France) were exposed to increasing concentrations of MeIQx and MeIQx-M1 and their impact on cell viability characterized as previously described (Zhang et al., 2017). Briefly, HepaRG cells were cultured in William's E medium (Thermo Scientific, Reinach, Switzerland) supplemented with 10% (*v*/v) fetal calf serum, 100 U ml^{-1} penicillin and 100 µg ml^{-1} streptomycin, 5 µg ml^{-1} insulin and 5×10^{-5} M hydrocortisone hemisuccinate. The cells were seeded in a 96-well-plate and grown for 2 weeks in media. For the following 2 weeks the cells were differentiated in medium containing 2% DMSO and then treated with MeIQx or MeIQx-M1 (0, 10, 50, 100, 150, 200, 350, 500, and 1250 µM in 0.5% DMSO from a 250-mM stock). The CellTiter-Glo® luminescent cell viability assay (Promega, Dübendorf, Switzerland) was then performed according to the manufacturer's protocol. As a positive control, 2% (v/v) Triton X-100 was used and the experiment was performed three times in total. The 10%-response benchmark dose (BMD_{10}) was calculated with PROAST (version 38.9) in R by following the manual provided by the European Food Safety Authority (EFSA; EFSA Scientific Committee, 2009).

2.8. Statistics

All statistical analyses were performed using GraphPad Prism (version 7.03; GraphPad, La Jolla, CA, USA). Multiple *t*-tests ($\alpha = 0.05$) were performed to compare the transport of MeIQx and MeIQx-M1 in different intestinal segments using the Holm-Sidak method. 2-way ANOVA multiple comparisons were performed to compare the cytotoxicity of MeIQx and MeIQx-M1. Outliers of apparent permeability (P_{app}) and fraction were identified using the ROUT method implemented in GraphPad Prism.

3. Results

3.1. Low transport of both MeIQx and its microbial metabolite through intestinal segments

To test the capacity of the rat intestine to transport MeIQx and its microbial metabolite MeIQx-M1, we added each to the mucosal compartment of an Ussing chamber and determined the amount of the chemical transported to the serosal compartment. The compounds were transported by all tissue segments. For MeIQx, levels in the serosal chamber ranged from 14.2 to 37.4 nM after 90 min (Fig. 2A and B) and proximal regions of the small and large intestine seemed to absorb more MeIQx when compared to their distal counterparts. For example, in the small intestine, the highest mean concentrations of MeIQx were observed in the proximal duodenum, followed by the proximal jejunum, ileum, and distal jejunum (Fig. 2A and B). A similar trend was observed in the large intestine, suggesting that the proximal region of the intestine might primarily contribute to the uptake of MeIQx. MeIQx-M1 was also slowly transported from the mucosal to the serosal compartment, and low levels were detected in the serosal chamber after 90 min of incubation, with the mean concentration values ranging from 7.9 to 10.8 nM (Fig. 2). No detectable amounts of MeIQx-M1 were measured in the serosal compartment after only 1 min of incubation. The concentrations of MeIQx-M1 in the mucosal compartments tended to decrease over time, although there were no significant differences in the levels of MeIQx-M1 in the mucosal compartment between 1 and 90 min after incubation (Fig. 2C and D). The tissues are viable throughout the 90-min experiment based on no significant changes on electrophysiological parameters such as the short-circuit current (I_{sc}) and tissue conductance (G_t; Table S5).

To address whether the microbial metabolism of MeIQx impacts its uptake, we quantitatively compared the intestinal uptake of MeIQx to

Table 1
Apparent permeability (P_{app}) and fraction of MeIQx/MeIQx-M1 absorbed by intestinal segments from rats.

Intestinal segment	Apparent permeability (P_{app}; $cm\,s^{-1} \times 10^{-6}$)		Fraction absorbed (%)	
	MeIQx	MeIQx-M1	MeIQx	MeIQx-M1
Duodenum	1.2 ± 1.4[a]	0.3 ± 0.3	0.3 ± 0.4	0.1 ± 0.1
Prox. jejunum	0.8 ± 0.8	0.3 ± 0.3	0.2 ± 0.2	0.1 ± 0.1
Dist. jejunum	0.6 ± 0.4	0.3 ± 0.3	0.1 ± 0.1	0.1 ± 0.1
Ileum	0.8 ± 0.4	0.3 ± 0.3	0.2 ± 0.1	0.1 ± 0.1
Caecum	1.2 ± 0.6	0.3 ± 0.4	0.3 ± 0.1	0.1 ± 0.1
Prox. colon	1.3 ± 0.8	0.3 ± 0.3	0.4 ± 0.2	0.1 ± 0.1
Dist. colon	0.7 ± 0.4	0.4 ± 0.4	0.2 ± 0.1	0.1 ± 0.1
Rectum	0.9 ± 0.6	0.3 ± 0.4	0.2 ± 0.2	0.1 ± 0.1

[a] Values are mean ± standard deviation of 4 to 6 animals.

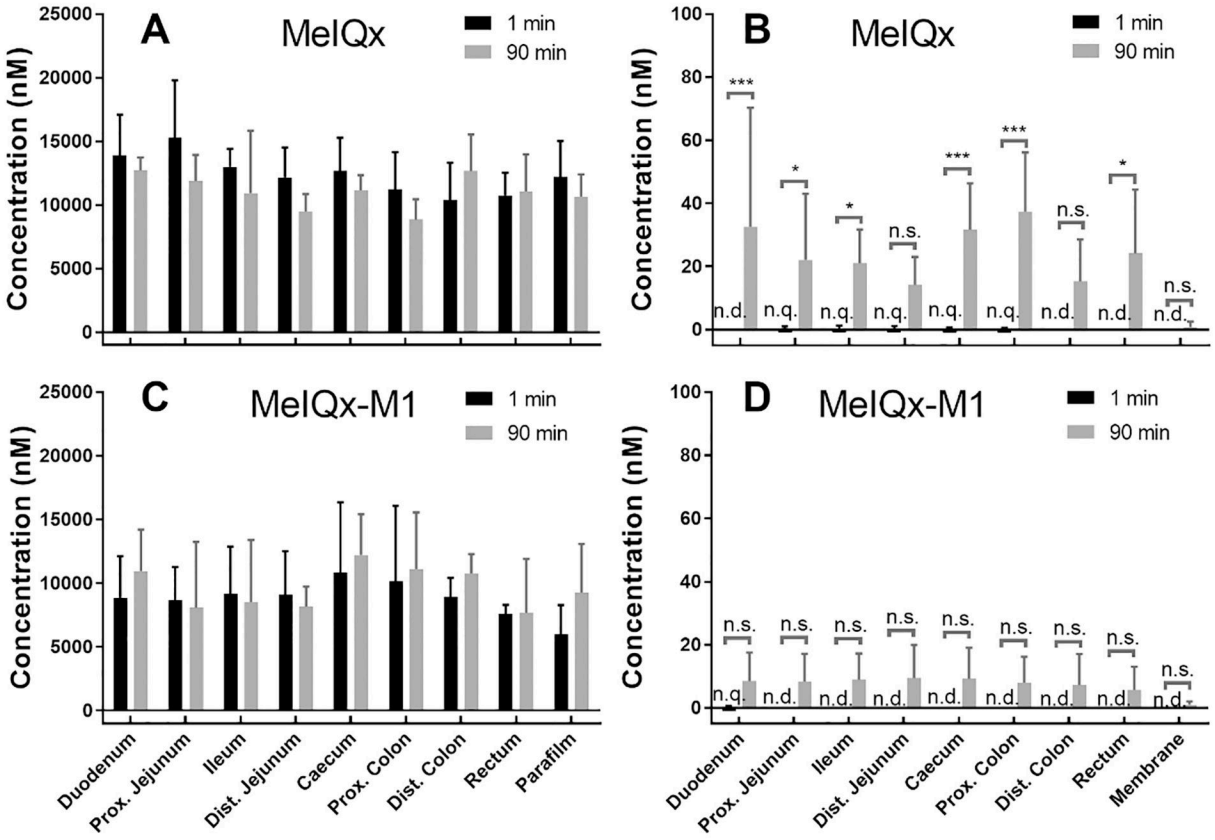

Fig. 2. Concentrations of MeIQx and MeIQx-M1 in the serosal and mucosal compartments of the Ussing chamber with clamped tissue samples from eight different rat intestinal segments. (A) Disappearance of MeIQx from the mucosal compartment. (B) Appearance of MeIQx in the serosal compartment. (C) Disappearance of MeIQx-M1 in the mucosal compartment. (D) Appearance of MeIQx in the serosal compartment. Error bars represent the standard deviation from at least three independent experiments analyzed in duplicate. $^{*}p < .05$; $^{***}p < .001$; n.s.: no significant differences detected; n.q.: not quantified; n.d.: not detected.

MeIQx-M1 by calculating the fraction of the compounds transported and the apparent permeability (P_{app}) for each in the different intestinal segments. The transport rate of MeIQx (0.1–0.4%) in all intestinal segments was slightly higher than for MeIQx-M1, which ranged from 0.06 to 0.09% (Table 1). Correspondingly, the P_{app} of MeIQx ($0.6–1.3 \times 10^{-6}$ cm s^{-1}) is greater than that of MeIQx-M1 ($0.3–0.4 \times 10^{-6}$ cm s^{-1}; Table 1).

3.2. Impact of MeIQx-M1 formation on the disposition of MeIQx via PBPK modeling

Having established that MeIQx and MeIQx-M1 are transported at similar rates, we aimed to estimate whether the microbial conjugation process has a significant influence on MeIQx disposition in humans. Therefore, we established a PBPK model wherein parameters were fit to in vivo plasma concentration data for MeIQx previously reported in 6 human subjects (Malfatti et al., 2016). We evaluated the performance of the model by comparing the fitted values of MeIQx plasma concentrations and the area under the curve (AUC) values with measured values from human subjects. The model satisfactorily simulated the kinetic profile of MeIQx in the different individuals (Figs. S5 and S6). Sensitivity analyses indicate that the AUC of MeIQx was highly sensitive to absorption rate, acrolein levels, glucuronidation, volume of GI tract, and body weight (Fig. S7). In the parameter fitting, we derived an estimated acrolein level for each individual that, based on the experimental uptake rates, could account for the measured MeIQx clearance rates (Table S6). Thereafter, batch runs were performed to compare the plasma levels of MeIQx in the presence and absence of acrolein. While the maximal plasma concentration (C_{max}) and AUC of MeIQx predicted using the model was not dramatically affected by the acrolein-mediated MeIQx transformation (up to 4-fold change, Table 2, Table S6), the plasma concentrations of MeIQx 4 or 8 h after its oral administration were dramatically decreased by up to 48-fold for all individuals. Correspondingly, up to 4005 μmoles acrolein were predicted to be required in these individuals for the microbial transformation to fully account for the loss pathway of the chemical.

3.3. Cytotoxicity of MeIQx and MeIQx-M1 in HepaRG cells

In a previous study, we found that MeIQx was more cytotoxic than MeIQx-M1 towards human colon epithelial cells, however, these cells are not metabolically competent and do not represent a physiologically relevant tissue site pertinent to when the compounds are taken up. Therefore, to test whether the microbial transformation has any impact on the cytotoxicity of MeIQx on metabolically competent liver cells, we exposed HepaRG cells to increasing concentrations of both compounds and evaluated cell viability. After 24 h exposure, neither induced cytotoxic effects at concentrations below or equal to 500 μM (Fig. S8). At the highest concentration tested, i.e. 1250 μM, MeIQx impaired cellular viability to a significantly greater extent than MeIQx-M1. Using these data, we calculated the benchmark dose (BMD), the no observed adverse effect level (NOAEL), and the lowest observed adverse effect level (LOAEL; Table 3), which were similar or slightly higher for MeIQx-M1 when compared to the values for MeIQx. The cytotoxicity data for the parent compound is consistent with data reported for MeIQx in HepaRG cells (Dumont et al., 2010), human liver cancer cells (Hep G2; Pezdirc et al., 2013), and non-malignantly transformed human colon epithelial cells (HCECs; Zhang et al., 2017).

Table 3
Cytotoxicity response of (μM) human liver HepaRG cells to MeIQx and the microbial metabolite MeIQx-M1.

Indicators[a]	Compounds		Fold reduction
	MeIQx (μM)	MeIQx-M1 (μM)	
$BMDL_{10}$	473	959	2
BMD_{10}	520	1195	2
$BMDU_{10}$	683	1229	2
NOAEL	500	500	1
LOAEL	1250	1250	1

[a] BMDL: lowest benchmark dose lower bound from Exponential models; BMD_{10}: benchmark dose with 10% benchmark response; BMDU: highest benchmark dose upper bound Hill models; NOAEL: no observed adverse effect level; LOAEL: lowest observed adverse effect level.

4. Discussion

The food carcinogen MeIQx can be metabolized to MeIQx-M1 by the microbial community in the human intestine. However, the influence of this microbial transformation process on systemic exposure remains unclear. The results of this study suggest that small percentages of MeIQx and MeIQx-M1 are transported from the mucosal to the serosal side of intestinal tissues. In addition, combining these transport values with previously reported plasma levels of MeIQx in humans, PBPK modeling showed that high levels of microbe-derived acrolein are required to reduce the systemic exposure of MeIQx in humans. Finally, it was confirmed that conversion of MeIQx to MeIQx-M1 does not likely induce liver toxicity after being taken up.

4.1. Conversion of MeIQx to MeIQx-M1 does not alter its transport rate

To evaluate the relevance of the MeIQx concentration used in the mucosal compartment, we considered the daily intake data available for MeIQx. The daily intake of MeIQx was estimated to range from 72 ng per day in Sweden (Augustsson et al., 1997) to 3.9 μg per day in Japan (Wakabayashi et al., 1997). The volume of the colon typically ranges

Table 2
Influence of bacteria-derived acrolein on the predicted plasma concentrations of MeIQx.

Subject[a]	Calculated acrolein level (μmoles)	C_{max}[b] ($\times 10^{-5}$ μM)			$C_{t=4h}$[b] ($\times 10^{-5}$ μM)			$C_{t=8h}$[b] ($\times 10^{-5}$ μM)			AUC_{0-8h}[b] ($\times 10^{-5}$ μM h)		
		N[c]	Y[c]	$Ratio_{N/Y}$[d]	N	Y	$Ratio_{N/Y}$	N	Y	$Ratio_{N/Y}$	N	Y	$Ratio_{N/Y}$
C1	1675	9.6	5.3	2	9.6	3.4	3	8.3	1.2	7	68.2	26.3	3
C2	2363	5.2	2.2	2	5.1	1.2	4	5.1	0.4	14	36.5	10.0	4
C3	3124	9.6	4.2	2	9.6	1.7	6	8.3	0.5	17	68.0	16.1	4
C4	2083	26.4	20.9	1	16.3	7.3	2	5.5	2.1	3	143.9	73.2	2
P3	2670	6.4	2.7	2	6.3	1.3	5	6.2	0.4	16	45.4	11.4	4
P4	4005	19.7	10.6	2	17.3	2.8	6	9.4	0.8	11	122.1	31.8	4

[a] C1–C4 and P3–P4 represent individual human subjects characterized in Malfatti et al. (2016).
[b] C_{max}, $C_{t=4\ h}$, $C_{t=8\ h}$ and $AUC_{0-8\ h}$ represent the plasma concentration of MeIQx at maxima, 4 h, 8 h as well as the area under the curve 8 h ($AUC_{0-8\ h}$) after compound administration, respectively.
[c] N and Y represent the PBPK-predicted plasma concentration of MeIQx in the absence and presence of indicated amount of acrolein in the PBPK model, respectively.
[d] The $ratio_{N/Y}$ is the indicator of the impact of acrolein (being further from 1.0 represents a higher influence on MeIQx plasma concentration).

from 160 to 203 ml in healthy subjects (Pritchard et al., 2014). Therefore, concentrations of MeIQx in the colon are estimated to range from 1.7 to 114 nM. Similarly, the concentration of dietary PhIP found in the colon is approximately 1.5–1.9 μM when considering a single dose of 70–84 μg administrated to human subjects (Malfatti et al., 2006) as well as the above-mentioned colon volume. Thus, the actual concentration of HCAs in the human gut after dietary intake of cooked meat is anticipated to be 1–3 orders of magnitude lower than the 10 μM used in the present study. Nevertheless, using 10 μM as the initial concentration allows for direct comparison with previous studies using 10 μM PhIP and PhIP-M1 to investigate the intestinal uptake of these compounds (Dietrich et al., 2001; Nicken et al., 2016, 2015, 2013, 2010).

The amount of MeIQx and MeIQx-M1 taken up after 90 min in the Ussing chamber model ranged from 0.1 to 0.4% and from 0.06 to 0.09%, respectively. These values are similar to what has been previously observed in the same model for the HCA PhIP and its analogous microbial metabolite PhIP-M1, i.e. 0.1–0.2% and 0.03–0.3%, respectively (Dietrich et al., 2001; Nicken et al., 2015, 2016;). While the model does not allow a direct comparison with in vivo data due to the small area of mucosal surface, limited period of time, and species-related differences, if the data is extrapolated on the basis of estimates for time of human intestinal transit (35 h) (Metcalf et al., 1987), and assuming similar transport rates for rat and human, the measured transport percentages would translate to up to 9% and 5% of MeIQx or PhIP, respectively, being taken up. In previous studies involving analysis of rat urine following oral MeIQx, Turesky et al. (1993) and Sjödin et al. (1989) reported slightly higher values of up to 20% and 41%, respectively. In these examples, the remaining chemical was excreted in the feces of the animals (Turesky et al., 1993; Sjödin et al., 1989). Similarly, Vanhaecke et al. found up to 21% of PhIP (unchanged plus acid-labile conjugates) excreted in urine, while up to 42% of PhIP was excreted in the feces from humans exposed to PhIP in food (Vanhaecke et al., 2008a). The potential underestimation of transport by the Ussing chamber model is consistent with a reported potential for underestimation by up to 5-fold observed in some cases that compared to single perfusion in vivo (Lennernäs, 2007). Despite the potential for underestimation of transport rates, the model is particularly effective for relative comparisons of chemicals vs. their metabolites.

The apparent permeability coefficients (P_{app}) for a wide range of compounds have been determined using the Ussing chamber to predict uptake or transport in the human intestine (Lennernäs, 2007). The P_{app} for HCAs and their microbial metabolites range from 0.3 to 1.2×10^{-6} cm s^{-1}, which is extremely low when compared to nutrients and some oral drugs such as D-glucose ($P_{app} = 100 \times 10^{-6}$ cm s^{-1}; human jejunal tissue; Sjöberg et al., 2013), naproxen ($P_{app} = 45 \times 10^{-6}$ cm s^{-1}; female Sprague-Dawley rat jejunum; Lennernäs et al., 1997) and ketoprofen ($P_{app} = 48 \times 10^{-6}$ cm s^{-1}, male Wistar rat jejunal tissue; Sjögren et al., 2016). In contrast, the P_{app} of some oral drugs such as fexofenadine and candesartan, which are only absorbed to a very limited extent, range from 0.8 to 1.2×10^{-6} cm s^{-1} (Sjögren et al., 2016), which is comparable to the P_{app} of MeIQx and MeIQx-M1 presented herein. While the intestinal transport is expected to occur in a manner that leads to a minor fraction impacting liver and other organs/tissues, due to the mutagenic basis of the mode of action of MeIQx following hepatic bioactivation, even low exposures may be physiologically relevant.

4.2. Bacteria-derived acrolein alters the MeIQx disposition in humans

Combining the transport values with previously reported plasma levels of MeIQx in humans, we established a PBPK model to evaluate the influence of bacteria-derived acrolein on the disposition of MeIQx in humans. Based on the prediction, the acrolein-mediated metabolic transformation of MeIQx in the intestine would decrease the AUC of MeIQx by 2 to 4-fold in six human individuals (Table 2). These results suggest that bacteria-derived acrolein may have a moderate influence on systemic exposure of MeIQx in human individuals. This prediction is consistent with an earlier observation by Vanhaecke et al. (2008b), that the efficiency of human fecal microbiota in converting PhIP to PhIP-M1 ranged from 2 to 98%. In addition, a great individual variation was also observed regarding the disposition and excretion of PhIP and PhIP-M1 in human subjects: While some individuals excreted a comparable amount of PhIP and PhIP-M1 in the urine, others excreted much more PhIP than PhIP-M1. Drawbacks of the present PBPK model might include the fact that the model calibration was only based on average anatomical parameters, albeit considering individual variations (Brown et al., 1997), as there is no information available on the physiological and anatomical parameters of the actual human subjects tested (Malfatti et al., 2016). Moreover, the established PBPK model did not include the detailed fate of acrolein in the gastrointestinal tract and considered the effective acrolein, but not free acrolein, available in that compartment. It has been shown that HCAs can be converted to M1 metabolites even when there is no detectable free acrolein in the solution (Engels et al., 2016), indicating that acrolein can exist in a conjugated form and retain reactivity. Hence, the calculated 4005 μmoles acrolein should be considered as acrolein equivalent, and thus a lower amount of free acrolein may be required to significantly influence MeIQx disposition. Moreover, the aforementioned potential for underestimation of transport rates in the Ussing chamber model translates to the potential for the present PBPK model to overestimate the required physiological acrolein equivalents required. Although there are many pieces of evidence indicating that acrolein is formed in the human gastrointestinal tract (Zhang et al., 2018), actual information on the levels and fate of this compound are not available.

5. Conclusions

In summary, we have demonstrated that MeIQx and its metabolite MeIQx-M1 have a similar intestinal transport rate and are not cytotoxic towards human liver hepaRG cells. PBPK modeling predicted that high levels of microbe-derived but not free acrolein may alter the systemic levels of MeIQx in humans by up to 4-fold. However, further studies are needed to validate the presented PBPK modeling on the basis of physiological acrolein levels, MeIQx transformation, and potentially higher absolute transport rates. The results infer that transformation by gut microbiota should be considered as a factor governing the disposition of dietary mutagenic HCAs in the human body. The PBPK model described here could be applied to other toxicants that are subjected to microbial transformation in order to be able to perform a more comprehensive and robust risk assessment of such compounds.

Conflict of interest

The authors declare no competing financial interests.

Acknowledgements

The authors wish to thank Marion Burmester and Kathrin Hansen for technical assistance during the Ussing chamber experiments, Prof. Karsten Beekmann for helpful discussion on PBPK modeling. This work was supported by the ETH Zürich (grant no. ETH-41 16-1 to SJS), EuroMix 633172-1 (SBFI No. 15.0115 to SJS), and the China Scholarship Council (grant no. 201406320209 to JZ).

Appendix A. Supplementary data

Supplementary data to this article can be found online at https://doi.org/10.1016/j.tiv.2019.04.004.

References

Al-malahmeh, A.J., Al-ajlouni, A., Wesseling, S., Soffers, E.M.F. Ans, Al-Subeihi, A., Kiwamoto, R., Vervoort, J., Rietjens, I.M.C.M., 2017. Physiologically based kinetic modeling of the bioactivation of myristicin. Arch. Toxicol. 91, 713–734.

Augustsson, K., Skog, K., Jägerstad, M., Steineck, G., 1997. Assessment of the human exposure to heterocyclic amines. Carcinogenesis 18, 1931–1935.

Beer, F., Urbat, F., Steck, J., Huch, M., Bunzel, D., Bunzel, M., Kulling, S.E., 2017. Metabolism of food-borne heterocyclic aromatic amines by *Lactobacillus reuteri* DSM 20016. J. Agric. Food Chem. 65, 6797–6811.

Behr, C., Kamp, H., Fabian, E., Krennrich, G., Mellert, W., Peter, E., Strauss, V., Walk, T., Rietjens, I.M.C.M., van Ravenzwaay, B., 2017. Gut microbiome-related metabolic changes in plasma of antibiotic-treated rats. Arch. Toxicol. 91, 3439–3454.

Bouvard, V., Loomis, D., Guyton, K.Z., Grosse, Y., Ghissassi, F. El, Benbrahim-Tallaa, L., Guha, N., Mattock, H., Straif, K., 2015. Carcinogenicity of consumption of red and processed meat. Lancet Oncol. 16, 1599–1600.

Breves, G., Walter, C., Burmester, M., Schröder, B., 2000. In vitro studies on the effects of *Saccharomyces boulardii* and *Bacillus cereus* var. toyoi on nutrient transport in pig jejunum. J. Anim. Physiol. Anim. Nutr. (Berl). 84, 9–20.

Brown, R.P., Delp, M.D., Lindstedt, S.L., Rhomberg, L.R., Beliles, R.P., 1997. Physiological paramter values for physiologically based pharmacokinetic models. Toxicol. Ind. Health 13, 407–484.

De Angelis, M., Bottacini, F., Fosso, B., Kelleher, P., Calasso, M., Di Cagno, R., Ventura, M., Picardi, E., Van Sinderen, D., Gobbetti, M., 2014. *Lactobacillus rossiae*, a vitamin B12 producer, represents a metabolically versatile species within the genus lactobacillus. PLoS One 9, 1–11.

DeJongh, J., Verhaar, H.J.M., Hermens, J.L.M., 1997. A quantitative property-property relationship (QPPR) approach to estimate in vitro tissue blood partition coefficients of organic chemicals in rats and humans. Arch. Toxicol. 72, 17–25.

Dietrich, C.G., de Waart, D.R., Ottenhoff, R., Schoots, I.G., Elferink, R.P., 2001. Increased bioavailability of the food-derived carcinogen 2-amino-1-methyl-6-phenylimidazo [4,5-*b*]pyridine in MRP2-deficient rats. Mol. Pharmacol. 59, 974–980.

Dumont, J., Jossé, R., Lambert, C., Anthérieu, S., Le Hegarat, L., Aninat, C., Robin, M.-A., Guguen-Guillouzo, C., Guillouzo, A., 2010. Differential toxicity of heterocyclic aromatic amines and their mixture in metabolically competent HepaRG cells. Toxicol. Appl. Pharmacol. 245, 256–263.

EFSA Scientific Committee, 2009. Guidance of the scientific committee on use of the benchmark dose approach in risk assessment. EFSA J. 1150, 1–72.

Engels, C., Schwab, C., Zhang, J., Stevens, M., Bieri, C., Ebert, M.-O., McNeill, K., Sturla, S.J., Lacroix, C., 2016. Acrolein contributes strongly to antimicrobial and heterocyclic amine transformation activities of reuterin. Sci. Rep. 6, 36246.

Fekry, M.I., Engels, C., Zhang, J., Schwab, C., Lacroix, C., Sturla, S.J., Chassard, C., 2016. The strict anaerobic gut microbe *Eubacterium hallii* transforms the carcinogenic dietary heterocyclic amine 2-amino-1-methyl-6-phenylimidazo[4,5-*b*]pyridine (PhIP). Environ. Microbiol. Rep. 8, 201–209.

Felton, J.S., Knize, M.G., Shen, N.H., Lewis, P.R., Andresen, B.D., Happe, J., Hatch, F.T., 1986. The isolation and identification of a new mutagen from fried ground beef: 2-amino-l-methyl-6-phenylimidazo [4, 5-*b*] pyridine (PhIP). Carcinogenesis 7, 1081–1086.

Haiser, H.J., Gootenberg, D.B., Chatman, K., Sirasani, G., Balskus, E.P., Turnbaugh, Peter J., 2013. Predicting and manipulating cardiac drug inactivation by the human gut bacterium *Eggerthella lenta*. Science 341, 295–298.

Humblot, C., Murkovic, M., Rigottier-Gois, L., Bensaada, M., Bouclet, A., Andrieux, C., Anba, J., Rabot, S., 2007. Beta-glucuronidase in human intestinal microbiota is necessary for the colonic genotoxicity of the food-borne carcinogen 2-amino-3-methylimidazo[4,5-*f*]quinoline in rats. Carcinogenesis 28, 2419–2425.

Ito, N., Hasegawa, R., Sano, M., Tamano, S., Esumi, H., Takayama, S., Sugimura, T., 1991. A new colon and mammary carcinogen in cooked food, 2-amino-1-methyl-6-phenylimidazo [4, 5-*b*] pyridine (PhIP). Carcinogenesis 12, 1503–1506.

Jägerstad, M., Olsson, K., Grivas, S., Negishi, C., Wakabayashi, K., Tsuda, M., Shigeaki, S., Takashi, S., 1984. Formation of 2-amino-3,8-dimethylimidazo[4,5-*f*]quinoxaline in a model system by heating creatinine, glycine and glucose. Mutat. Res. Fundam. Mol. Mech. Mutagen. 126, 239–244.

Kasai, H., Yamaizumi, Z., Wakabayashi, K., Nagao, M., Sugimura, T., Yokoyama, S., Miyazawa, T., Spingarn, N.E., Weisburger, J.H., Nishimura, S., 1980. Potent novel mutagens produced by broiling fish under normal conditions. Proc. Japan Acad. Ser. B 56, 278–283.

Kato, T., Ohgaki, H., Hasegawa, H., Sato, S., Takayama, S., Sugimura, T., 1988. Carcinogenicity in rats of a mutagenic compound, 2-amino-3,8-dimethylimidazo[4,5-*f*]quinoxaline. Carcinogenesis 9, 71–73.

Kim, D., Guengerich, F.P., 2005. Cytochrome P450 activation of arylamines and heterocyclic amines. Annu. Rev. Pharmacol. Toxicol. 45, 27–49.

Lennernäs, H., 2007. Animal data: the contributions of the Ussing chamber and perfusion systems to predicting human oral drug delivery in vivo. Adv. Drug Deliv. Rev. 59, 1103–1120.

Lennernäs, H., Nylander, S., Ungell, A.-L., 1997. Jejunal permeability: a comparison between the Ussing chamber technique and the single-pass perfusion in humans. Pharm. Res. 14, 667–671.

Malfatti, M.A., Felton, J.S., 2004. Human UDP-glucuronosyltransferase 1A1 is the primary enzyme responsible for the *N*-glucuronidation of *N*-hydroxy-PhIP in vitro. Chem. Res. Toxicol. 17, 1137–1144.

Malfatti, M.A., Dingley, K.H., Nowell-Kadlubar, S., Ubick, E.A., Mulakken, N., Nelson, D., Lang, N.P., Felton, J.S., Turteltaub, K.W., 2006. The urinary metabolite profile of the dietary carcinogen 2-amino-1-methyl-6-phenylimidazo[4,5-*b*]pyridine is predictive of colon DNA adducts after a low-dose exposure in humans. Cancer Res. 66, 10541–10547.

Malfatti, M.A., Kuhn, E.A., Turteltaub, K.W., Vickers, S.M., Jensen, E.H., Strayer, L., Anderson, K.E., 2016. Disposition of the dietary mutagen 2-amino-3,8-dimethylimidazo[4,5-*f*]quinoxaline in healthy and pancreatic cancer compromised humans. Chem. Res. Toxicol. 29, 352–358.

Metcalf, A.M., Phillips, S.F., Zinsmeister, A.R., MacCarty, R.L., Beart, R.W., Wolff, B.G., 1987. Simplified assessment of segmental colonic transit. Gastroenterology 92, 40–47.

Nauwelaers, G., Bessette, E.E., Gu, D., Tang, Y., Rageul, J., Fessard, V., Yuan, J.-M., Yu, M.C., Langouët, S., Turesky, R.J., 2011. DNA adduct formation of 4-aminobiphenyl and heterocyclic aromatic amines in human hepatocytes. Chem. Res. Toxicol. 24, 913–925.

Nicken, P., Hamscher, G., Breves, G., Steinberg, P., 2010. Uptake of the colon carcinogen 2-amino-1-methyl-6-phenylimidazo[4,5-*b*]pyridine by different segments of the rat gastrointestinal tract: its implication in colorectal carcinogenesis. Toxicol. Lett. 196, 60–66.

Nicken, P., Schröder, B., von Keutz, A., Breves, G., Steinberg, P., 2013. The colon carcinogen 2-amino-1-methyl-6-phenylimidazo [4, 5-*b*] pyridine (PhIP) is actively secreted in the distal colon of the rat: an integrated view on the role of PhIP transport and metabolism in PhIP-induced colon carcinogenesis. Arch. Toxicol. 87, 895–904.

Nicken, P., Willenberg, I., Keutz, A. von, Elsner, L. von, Hamscher, G., Vanhaecke, L., Schröder, B., Breves, G., Schebb, N.H., Steinberg, P., 2015. Intestinal absorption and cell transforming potential of PhIP-M1, a bacterial metabolite of the heterocyclic aromatic amine 2-amino-1-methyl-6-phenylimidazo[4,5-*b*]pyridine (PhIP). Toxicol. Lett. 234, 92–98.

Nicken, P., von Keutz, A., Willenberg, I., Ostermann, A.I., Schebb, N.H., Giovannini, S., Kershaw, O., Breves, G., Steinberg, P., 2016. Impact of dextran sulphate sodium-induced colitis on the intestinal transport of the colon carcinogen PhIP. Arch. Toxicol. 90, 1093–1102.

Ohgaki, H., Hasegawa, H., Suenaga, M., Sato, S., Takayama, S., Sugimura, T., 1987. Carcinogenicity in mice of a mutagenic compound, 2-amino-3,8-dimethylimidazo [4,5-*f*]quinoxaline (MeIQx) from cooked foods. Carcinogenesis 8, 665–668.

Ozawa, S., Nagata, K., Yamazoe, Y., Kato, R., 1995. Formation of 2-amino-3-methylimidazo[4,5-*f*]quinoline- and 2-amino-3,8-dimethylimidazo[4,5-*f*]quinoxaline-sulfamates by cDNA-expressed mammalian phenol sulfotransferases. Jpn. J. Cancer Res. 86, 264–269.

Pezdirc, M., Žegura, B., Filipič, M., 2013. Genotoxicity and induction of DNA damage responsive genes by food-borne heterocyclic aromatic amines in human hepatoma HepG2 cells. Food Chem. Toxicol. 59, 386–394.

Pfau, W., Martin, F.L., Cole, K.J., Venitt, S., Phillips, D.H., Grover, P.L., Marquardt, H., 1999. Heterocyclic aromatic amines induce DNA strand breaks and cell transformation. Carcinogenesis 20, 545–551.

Pritchard, S.E., Marciani, L., Garsed, K.C., Hoad, C.L., Thongborisute, W., Roberts, E., Gowland, P.A., Spiller, R.C., 2014. Fasting and postprandial volumes of the undisturbed colon: Normal values and changes in diarrhea-predominant irritable bowel syndrome measured using serial MRI. Neurogastroenterol. Motil. 26, 124–130.

Rendic, S., Guengerich, F.P., 2012. Contributions of human enzymes in carcinogen metabolism. Chem. Res. Toxicol. 25, 1316–1383.

Sinha, R., Kulldorff, M., Chow, W.H., Denobile, J., Rothman, N., 2001. Dietary intake of heterocyclic amines, meat-derived mutagenic activity, and risk of colorectal adenomas. Cancer Epidemiol. Biomark. Prev. 10, 559–562.

Sjöberg, Å., Lutz, M., Tannergren, C., Wingolf, C., Borde, A., Ungell, A.L., 2013. Comprehensive study on regional human intestinal permeability and prediction of fraction absorbed of drugs using the Ussing chamber technique. Eur. J. Pharm. Sci. 48, 166–180.

Sjödin, P., Wallin, H., Alexander, J., Jägerstad, M., 1989. Disposition and metabolism of the food mutagen 2-amino-3,8-dimethylimidazo[4, 5-*f*]quinoxaline (MeIQx) in rats. Carcinogenesis 10, 1269–1275.

Sjögren, E., Eriksson, J., Vedin, C., Breitholtz, K., Hilgendorf, C., 2016. Excised segments of rat small intestine in Ussing chamber studies: a comparison of native and stripped tissue viability and permeability to drugs. Int. J. Pharm. 505, 361–368.

Spanogiannopoulos, P., Bess, E.N., Carmody, R.N., Turnbaugh, P.J., 2016. The microbial pharmacists within us: a metagenomic view of xenobiotic metabolism. Nat. Rev. Microbiol. 14 (5), 273–287.

Sugimura, T., 1988. Successful use of short-term tests for academic purposes: their use in identification of new environmental carcinogens with possible risk for humans. Mutat. Res. 205, 33–39.

Sugimura, T., Wakabayashi, K., Nakagama, H., Nagao, M., 2004. Heterocyclic amines: mutagens/carcinogens produced during cooking of meet and fish. Cancer Sci. 95, 290–299.

Tóth, B., 2007. Association between Electrophysiological Phenotype and Genotype in the Cftr TgH (Neoim) Hgu Mouse Model.

Turesky, R.J., Stillwell, W.G.S., Skipper, P.L., Tannenbaum, S.R., 1993. Metabolism of the food-borne carcinogens 2-amino-3-methylimidazo[4,5-*f*]quinoline and 2-amino-3,8-dimethylimidazo[4,5-*f*]-quinoxaline in the rat as a model for human biomonitoring. Environ. Health Perspect. 99, 123–128.

Ushiyama, H., Wakabayashi, K., Hirose, M., Itoh, H., Sugimura, T., Nagao, M., 1991. Presence of carcinogenic heterocyclic amines in urine of healthy volunteers eating normal diet, but not of inpatients receiving parenteral alimentation. Carcinogenesis 12, 1417–1422.

Vanhaecke, L., Van Hoof, N., Van Brabandt, W., Soenen, B., Heyerick, A., De Kimpe, N., De Keukeleire, D., Verstraete, W., Van de Wiele, T., 2006. Metabolism of the food-associated carcinogen 2-amino-1-methyl-6-phenylimidazo[4,5-*b*]pyridine by human intestinal microbiota. J. Agric. Food Chem. 54, 3454–3461.

Vanhaecke, L., Knize, M.G., Noppe, H., Brabander, H. De, Verstraete, W., Van de Wiele, T., 2008a. Intestinal bacteria metabolize the dietary carcinogen 2-amino-1-methyl-6-

phenylimidazo[4,5-*b*]pyridine following consumption of a single cooked chicken meal in humans. Food Chem. Toxicol. 46, 140–148.
Vanhaecke, L., Vercruysse, F., Boon, N., Verstraete, W., Cleenwerck, I., De Wachter, M., De Vos, P., van de Wiele, T., 2008b. Isolation and characterization of human intestinal bacteria capable of transforming the dietary carcinogen 2-amino-1-methyl-6-phenylimidazo[4,5-*b*]pyridine. Appl. Environ. Microbiol. 74, 1469–1477.
Wakabayashi, K., Totsuka, Y., Fukutome, K., Oguri, A., Ushiyama, H., Sugimura, T., 1997. Human exposure to mutagenic/carcinogenic heterocyclic amines and comutagenic beta-carbolines. Mutat. Res. Fundam. Mol. Mech. Mutagen. 376, 253–259.
Yee, S., 1997. In vitro permeability across Caco-2 cells (colonic) can predict *in vivo* (small intestinal) absorption in man - fact or myth. Pharm. Res. 14 (6), 763–766.
Zhang, J., Empl, M.T., Schwab, C., Fekry, M.I., Engels, C., Schneider, M., Lacroix, C., Steinberg, P., Sturla, S.J., 2017. Gut microbial transformation of the dietary imidazoquinoxaline mutagen MeIQx reduces its cytotoxic and mutagenic potency. Toxicol. Sci. 159, 266–276.
Zhang, J., Sturla, S.J., Lacroix, C., Schwab, C., 2018. Gut microbial glycerol metabolism as an endogenous acrolein source. MBio 9 e01947–17.
Zhou, H., Josephy, P.D., Kim, D., Guengerich, F.P., 2004. Functional characterization of four allelic variants of human cytochrome P450 1A2. Arch. Biochem. Biophys. 422, 23–30.